



Research article

Solution structure and stability for a two-parameter acoustic inverse scattering problem

Jing Xu¹, Jingzhi Li^{2,*}, Yan Chang³ and Tian Niu⁴

¹ School of Statistics and Mathematics & Research Center for Regional Digital Economy and Digital Governance, Inner Mongolia University of Finance and Economics, Hohhot 010070, China

² Department of Mathematics & National Center for Applied Mathematics Shenzhen & SUSTech, International Center for Mathematics, Southern University of Science and Technology, Shenzhen 518055, China

³ School of Mathematics & School of Physics, Harbin Institute of Technology, Harbin 150001, China

⁴ Department of Mathematics, Southern University of Science and Technology, Shenzhen 518055, China

* **Correspondence:** Email: li.jz@sustech.edu.cn.

Abstract: This paper investigated the structure and stability of solutions for simultaneously recovering density and bulk modulus in acoustic inverse scattering. The nonlinear scattering model was linearized via the Born approximation, and the inverse problem was casted as a 2×2 block operator equation. The off-diagonal blocks of this operator matrix captured the cross-coupling interactions between the two physical parameters. By employing the maximal Tseng generalized inverse, we developed an analytical formulation that remained valid even when diagonal blocks were non-invertible, overcoming limitations of traditional Schur complement methods. To address the inherent ill-posedness, we incorporated Tikhonov regularization into this linearized system, deriving explicit solution representations and establishing a rigorous stability estimate. Our analysis revealed that the strength of the off-diagonal interaction imposed a fundamental lower bound on the regularization parameter. As the parameter approached this bound, the reconstruction error exhibited singular behavior.

Keywords: acoustic inverse scattering; multi-parameter inversion; maximal Tseng generalized inverse; Tikhonov regularization; stability estimate

1. Introduction

Inverse scattering problems constitute a central topic in applied mathematics and physics, with wide-ranging applications including radar and sonar target identification, medical ultrasound computed tomography (CT), geophysical exploration, and nondestructive evaluation [1–3]. The fundamental objective of these problems is the quantitative reconstruction of the physical properties or geometric features of an unknown scatterer from measured scattered field data. However, such problems are intrinsically nonlinear and ill-posed, posing significant challenges for theoretical analysis and numerical computation.

To address the intrinsic nonlinearity and ill-posedness, regularization theory coupled with linearization strategies has been extensively investigated. A widely adopted approach involves linearizing the nonlinear forward map via strategies such as the Born, Rytov, or Kirchhoff approximations [1, 4], as well as Newton-type iterative schemes [5, 6]. Following linearization, regularization techniques become essential to handle the severe ill-conditioning of the resulting system. The most fundamental strategy is Tikhonov regularization, systematically detailed in [7], which stabilizes the inversion by minimizing a functional balancing data fidelity with a penalty term. This method provides a robust framework with well-established theories on existence, stability, and convergence rates [8, 9]. Beyond the classical Tikhonov framework, alternative strategies include iterative regularization methods [10, 11], iteratively regularized Gauss-Newton schemes [5], and sparsity-promoting techniques [12].

As an intrinsically nonlinear and ill-posed problem, the inverse medium scattering problem has been extensively investigated. Methodologies range from iterative regularization for strong scattering [13], to comprehensive analyses of Tikhonov-type schemes [2, 14], and even globally convex formulations based on Carleman estimates [15, 16]. While these contributions have significantly advanced the field, most focus on single-parameter models. However, characterizing realistic acoustic media requires the simultaneous determination of both density and bulk modulus.

Simultaneous reconstruction of multiple parameters is a formidable challenge. The literature shows that uniqueness for such co-inversion problems often requires strong prior assumptions or supplementary data. For example, uniqueness was established for recovering a piecewise constant medium with an embedded object [17]. Other studies prove uniqueness for an obstacle and its sources by using additional data to decouple the problem [18, 19]. Even advanced algorithms may need partial a priori information to handle these coupled systems effectively [20]. These works collectively demonstrate that the coupling in multiparameter problems presents a fundamental theoretical challenge. This difficulty in the full nonlinear setting motivates a rigorous analysis of the linearized problem, which is often the basis for practical inversion algorithms.

This challenge is particularly evident in the dual-parameter acoustic inversion problem, which has numerous applications in fields such as medical ultrasound tomography [21] and geophysical full-waveform inversion [22, 23]. In these applications, the contributions of density and modulus variations are intertwined in the scattering data, creating a composite source term that exacerbates the problem's ill-posedness. Standard decoupled strategies often fail to separate these coupled contributions, leading to significant artifacts in the reconstructed images [24]. While multiparameter regularization techniques have been explored to address this issue [14, 25], they typically rely on the assumption that the forward operator is well-behaved. However, in scenarios where certain modes of the contrast are unobservable, such as in limited-aperture or low-frequency measurements, the

resulting normal operator exhibits structural singularities, specifically manifested as non-invertible diagonal blocks. In such cases, classical block inversion methods based on the Schur complement become inapplicable.

To address this challenge, this paper analyzes the structure and stability of the solution based on the theory of the maximal Tseng generalized inverse. Instead of the spectral analysis for one-sided coupled matrices [26–28], we establish here the explicit solution structure for general 2×2 operator matrices. After linearizing the problem into a 2×2 block operator equation using the Born approximation, we derive an explicit analytical representation for its generalized inverse. This representation decomposes the solution operator in terms of its diagonal and off-diagonal blocks, explicitly showing how parameter coupling affects the solution. Building on this analysis, we then investigate the Tikhonov-regularized problem and establish a rigorous stability estimate. This estimate reveals that the strength of the parameter coupling fundamentally dictates a critical lower bound for the regularization parameter, and that the reconstruction error exhibits singular behavior as this bound is approached. Crucially, our approach does not require the diagonal blocks to be invertible, making it applicable to structurally singular systems where traditional methods based on the Schur complement fail.

This paper is organized as follows. Section 2 formulates the mathematical model for the two-parameter acoustic inverse scattering problem, derives the Lippmann-Schwinger equation under the Born approximation, and introduces the resulting block operator structure. Section 3 develops the theory of the Tseng generalized inverse and presents our main theorem concerning the inverse of a perturbed block operator. Section 4 applies this theorem to the Tikhonov-regularized system, providing a detailed analysis of the solution's structure and stability. In Section 5, we provide a summary of our findings and discuss the outlook for future work.

2. The two-parameter acoustic inverse scattering problem

This section provides a detailed mathematical formulation for a canonical two-parameter acoustic scattering problem. The resulting framework, culminating in a precise 2×2 block operator system, serves as a concrete foundation for the theoretical analysis presented in the subsequent sections.

2.1. The direct scattering problem

Assume that the space \mathbb{R}^3 is filled with a homogeneous and non-dissipative medium, characterized by a constant density ρ_0 and a constant bulk modulus κ_0 . Under the time-harmonic assumption, the linearized acoustic wave equation reduces to the homogeneous Helmholtz equation [1, Section 2.1]. The incident field $u^{\text{inc}}(x)$ satisfies

$$\Delta u^{\text{inc}}(x) + k_0^2 u^{\text{inc}}(x) = 0 \quad \text{in } \mathbb{R}^3, \quad (2.1)$$

where the wave number $k_0 > 0$ is related to the angular frequency ω by

$$k_0^2 = \frac{\omega^2 \rho_0}{\kappa_0}. \quad (2.2)$$

Let the scatterer be an inhomogeneous medium characterized by its density $\rho(x)$ and bulk modulus $\kappa(x)$. The scatterer is assumed to have a compact support $\overline{\Omega}$, where $\Omega \subset \mathbb{R}^3$ is a bounded, open domain

with a C^2 boundary. The physical parameters coincide with the background constants (ρ_0, κ_0) for all $x \in \mathbb{R}^3 \setminus \overline{\Omega}$. The direct scattering problem is to find the total field $u = u^{\text{inc}} + u^s$ such that $u \in H_{\text{loc}}^1(\mathbb{R}^3)$ satisfies the Helmholtz equation governing acoustic propagation in an inhomogeneous medium. We introduce the contrast functions $m_\rho(x)$ and $m_\kappa(x)$, defined in terms of the density and bulk modulus as

$$m_\rho(x) := 1 - \frac{\rho_0}{\rho(x)} \quad \text{and} \quad m_\kappa(x) := 1 - \frac{\kappa_0}{\kappa(x)}. \quad (2.3)$$

Following the standard derivation in [1, Section 8.1], we rewrite the acoustic wave equation in terms of the background wave number k_0 and these contrast functions as

$$\Delta u(x) + k_0^2 u(x) = \nabla \cdot (m_\rho(x) \nabla u(x)) + k_0^2 m_\kappa(x) u(x) \quad \text{in} \quad \mathbb{R}^3, \quad (2.4)$$

where the scattered field u^s satisfies the Sommerfeld radiation condition

$$\lim_{r \rightarrow \infty} r \left(\frac{\partial u^s}{\partial r} - ik_0 u^s \right) = 0, \quad \text{where } r = |x|. \quad (2.5)$$

The well-posedness of this forward scattering problem is a classical result in scattering theory, typically established by reformulating the problem as an integral equation [1, 29]. If the density is constant, i.e., $\rho(x) \equiv \rho_0$, then $\nabla \cdot (m_\rho \nabla u)$ vanishes, and Eq (2.4) reduces to the classical medium scattering equation. The inverse problem is then to reconstruct the pair of functions, which we represent by the vector $\mathbf{m}(x) = (m_\rho(x), m_\kappa(x))^T$ from scattering measurements.

2.2. The Lippmann-Schwinger equation and the Born approximation

The governing partial differential equation (PDE) (2.4) coupled with the radiation condition (2.5) is equivalently reformulated as the Lippmann-Schwinger integral equation for the total field u :

$$u = u^{\text{inc}} - \int_{\Omega} \Phi(x, y) \left(\nabla_y \cdot (m_\rho(y) \nabla_y u(y)) + k_0^2 m_\kappa(y) u(y) \right) dy, \quad (2.6)$$

where $\Phi(x, y)$ is the Green's function, given by

$$\Phi(x, y) = \frac{e^{ik_0|x-y|}}{4\pi|x-y|}. \quad (2.7)$$

The equation remains nonlinear due to the presence of the total field $u = u^{\text{inc}} + u^s$ within the source term on the righthand side.

To obtain a linear equation, we apply the first-order Born approximation. Under the assumption of weak scattering (i.e., $|u^s| \ll |u^{\text{inc}}|$), we replace the total field u inside the integral with the known incident field u^{inc} . This linearization yields the linear integral equation:

$$u_{\text{Born}}^s(x) = - \int_{\Omega} \Phi(x, y) \nabla_y \cdot (m_\rho(y) \nabla_y u^{\text{inc}}(y)) dy - k_0^2 \int_{\Omega} \Phi(x, y) m_\kappa(y) u^{\text{inc}}(y) dy, \quad (2.8)$$

where u_{Born}^s denotes the Born-approximated scattered field. This defines the linearized problem under the Born approximation with higher-order scattering effects contributing errors of order $O(\|\mathbf{m}\|^2)$. By

applying Green's first identity and using the compact support of m_ρ in Ω to eliminate the boundary integral, the first term in (2.8) is transformed into

$$\int_{\Omega} \Phi(x, y) \nabla_y \cdot (m_\rho(y) \nabla_y u^{\text{inc}}(y)) dy = - \int_{\Omega} \nabla_y \Phi(x, y) \cdot (m_\rho(y) \nabla_y u^{\text{inc}}(y)) dy. \quad (2.9)$$

Substituting this identity back into (2.8), we arrive at the final form of the linearized integral equation

$$u_{\text{Born}}^s(x) = \int_{\Omega} (\nabla_y \Phi(x, y) \cdot \nabla_y u^{\text{inc}}(y)) m_\rho(y) dy - k_0^2 \int_{\Omega} \Phi(x, y) u^{\text{inc}}(y) m_\kappa(y) dy. \quad (2.10)$$

This equation provides an explicit linear relationship between the contrast functions $\mathbf{m} = (m_\rho, m_\kappa)^\top$ and the Born-approximated scattered field.

We define the two linear integral operators \mathcal{J}_ρ and \mathcal{J}_κ by

$$(\mathcal{J}_\rho m_\rho)(x) := \int_{\Omega} (\nabla_y \Phi(x, y) \cdot \nabla_y u^{\text{inc}}(y)) m_\rho(y) dy, \quad (2.11)$$

$$(\mathcal{J}_\kappa m_\kappa)(x) := -k_0^2 \int_{\Omega} \Phi(x, y) u^{\text{inc}}(y) m_\kappa(y) dy, \quad (2.12)$$

and the block operator $\mathcal{J} = \begin{pmatrix} \mathcal{J}_\rho & \mathcal{J}_\kappa \end{pmatrix}$. The linearized problem (2.10) can then be written as

$$u_{\text{Born}}^s(x) = (\mathcal{J} \mathbf{m})(x). \quad (2.13)$$

The linear operator $\mathcal{J} : L^2(\Omega) \times L^2(\Omega) \rightarrow L^2(\Gamma)$ maps the space of contrast functions to the space of the Born-approximated scattered field on Γ .

2.3. The block operator structure

In the practical inverse problem, we aim to reconstruct the vector \mathbf{m} from measurements of the scattered field u_{obs} . This observed data is inevitably corrupted by measurement noise and subject to errors inherent in the Born approximation. The solution is therefore sought by minimizing the squared norm of the residual, which is defined as

$$\min_{\mathbf{m}} \|\mathcal{J} \mathbf{m} - u_{\text{obs}}\|^2. \quad (2.14)$$

Solving this least-squares problem is equivalent to solving the equation

$$\mathcal{J}^* \mathcal{J} \mathbf{m} = \mathcal{J}^* u_{\text{obs}}, \quad (2.15)$$

where $\mathcal{J}^* : L^2(\Gamma) \rightarrow L^2(\Omega) \times L^2(\Omega)$ is the adjoint of \mathcal{J} .

The operator \mathcal{J} has a 1×2 block structure given by $\mathcal{J} = \begin{pmatrix} \mathcal{J}_\rho & \mathcal{J}_\kappa \end{pmatrix}$. Consequently, its adjoint \mathcal{J}^* has the corresponding 2×1 block structure

$$\mathcal{J}^* = \begin{pmatrix} \mathcal{J}_\rho^* \\ \mathcal{J}_\kappa^* \end{pmatrix}. \quad (2.16)$$

By direct block operator multiplication, we have

$$\mathcal{M} = \begin{pmatrix} \mathcal{J}_\rho^* \\ \mathcal{J}_\kappa^* \end{pmatrix} (\mathcal{J}_\rho \quad \mathcal{J}_\kappa) = \begin{pmatrix} \mathcal{J}_\rho^* \mathcal{J}_\rho & \mathcal{J}_\rho^* \mathcal{J}_\kappa \\ \mathcal{J}_\kappa^* \mathcal{J}_\rho & \mathcal{J}_\kappa^* \mathcal{J}_\kappa \end{pmatrix} =: \begin{pmatrix} A & B \\ C & D \end{pmatrix}. \quad (2.17)$$

Here, the diagonal operators A and D are associated with the inverse problem for each parameter individually, while the off-diagonal operators B and C represent the coupling between the density and bulk modulus contrasts. The stability of the joint inversion generally improves as the diagonal operators become better-conditioned and the norms of the off-diagonal coupling operators decrease [22, 30]. The operator $\mathcal{M} : L^2(\Omega) \times L^2(\Omega) \rightarrow L^2(\Omega) \times L^2(\Omega)$ is thus represented by the block matrix in (2.17).

In this paper, we provide a representation for the solution of the following ill-posed equation

$$\mathcal{M}m = \mathcal{J}^* u_{\text{obs}} \quad (2.18)$$

by employing the maximal Tseng generalized inverse of the operator matrix \mathcal{M} .

3. Theory of perturbed block operators and their generalized inverses

Let X and Y be Hilbert spaces. We denote by $\mathcal{L}(X, Y)$ the space of all linear operators from X to Y , and by $\mathcal{B}(X, Y)$ the space of all bounded linear operators. Furthermore, let $\mathcal{C}(X, Y)$ denote the set of all densely defined, closed linear operators from X to Y . When $Y = X$, we adopt the shorthand notations $\mathcal{L}(X)$, $\mathcal{C}(X)$, and $\mathcal{B}(X)$. The domain, kernel (or null space), and range of an operator T are denoted by $\mathcal{D}(T)$, $\mathcal{N}(T)$, and $\mathcal{R}(T)$, respectively.

Definition 1 (see [31]). *Let T and S be linear operators with the same domain space. The operator S is said to be T -bounded if $\mathcal{D}(T) \subset \mathcal{D}(S)$ and there exist nonnegative constants a, b such that*

$$\|Su\| \leq a\|u\| + b\|Tu\|, \quad u \in \mathcal{D}(T). \quad (3.1)$$

The greatest lower bound of all possible constants b is called the T -bound of S .

Definition 2 (see [32]). *Let $T \in \mathcal{L}(X, Y)$. An operator $S \in \mathcal{L}(Y, X)$ is a Tseng generalized inverse of T , if $\mathcal{R}(T) \subset \mathcal{D}(S)$, $\mathcal{R}(S) \subset \mathcal{D}(T)$, and ST and TS are, respectively, the following restrictions:*

$$ST = P_{\overline{\mathcal{R}(S)}}|_{\mathcal{D}(T)}, \quad TS = P_{\overline{\mathcal{R}(T)}}|_{\mathcal{D}(S)}. \quad (3.2)$$

Here $P_{\overline{\mathcal{R}(S)}}$ and $P_{\overline{\mathcal{R}(T)}}$ are orthogonal projections onto $\overline{\mathcal{R}(S)}$ and onto $\overline{\mathcal{R}(T)}$, respectively.

It is well known that an operator T has a Tseng generalized inverse if, and only if, the domain of T admits the decomposition

$$\mathcal{D}(T) = \mathcal{N}(T) \oplus (\mathcal{D}(T) \cap \mathcal{N}(T)^\perp). \quad (3.3)$$

When this condition holds, the range of any Tseng generalized inverse S of T is given by $\mathcal{R}(S) = \mathcal{D}(T) \cap \mathcal{N}(T)^\perp$, and the null space of S can be any subspace of $\mathcal{R}(T)^\perp$. This decomposition of the domain is satisfied for any $T \in \mathcal{C}(X, Y)$ or $T \in \mathcal{B}(X, Y)$, since the kernel of T is closed.

Definition 3 (see [32]). *The maximal Tseng generalized inverse T^\dagger of an operator $T \in \mathcal{L}(X, Y)$ is the Tseng generalized inverse of T with $\mathcal{D}(T^\dagger) = \mathcal{R}(T) \oplus \mathcal{R}(T)^\perp$ and $\mathcal{N}(T^\dagger) = \mathcal{R}(T)^\perp$.*

Lemma 1 (see [32]). *Let $T \in C(X, Y)$. Then, the following hold:*

- (i) $(T^\dagger)^\dagger = T$ and $\mathcal{N}(T) = \mathcal{R}(T^\dagger)^\perp$.
- (ii) $\mathcal{R}(T)$ is closed if, and only if, $T^\dagger \in \mathcal{B}(Y, X)$.

We begin our theoretical analysis with a key proposition concerning the generalized inverse of perturbed operators. This result will serve as the cornerstone for the proofs of our main theorems.

Proposition 1. *Consider an operator $T \in C(X, Y)$ with a closed range $\mathcal{R}(T)$, and a T -bounded perturbation $\delta T \in \mathcal{L}(X, Y)$. Let the perturbed operator be defined as $\bar{T} = T + \delta T$. Assume that $(I + \delta T T^\dagger)$ is a bijective operator. Then, the perturbed operator \bar{T} is a closed operator and its maximal Tseng generalized inverse is given by the formula*

$$\bar{T}^\dagger = T^\dagger (I + \delta T T^\dagger)^{-1}, \quad (3.4)$$

if, and only if, the null space and range of the perturbation δT are related to those of T by the inclusions

$$\mathcal{N}(T) \subset \mathcal{N}(\delta T) \quad \text{and} \quad \mathcal{R}(\delta T|_{\mathcal{D}(T)}) \subset \mathcal{R}(T). \quad (3.5)$$

In this case, the range $\mathcal{R}(\bar{T})$ is also closed.

Proof. On the one hand, for $y \in \mathcal{R}(T^\dagger)$, there exists $x \in \mathcal{D}(T^\dagger) = Y$ such that $y = T^\dagger x$. Since $I + \delta T T^\dagger$ is bijective, we have $x \in \mathcal{R}((I + \delta T T^\dagger)^{-1})$, then $y = T^\dagger x \in \mathcal{R}(T^\dagger (I + \delta T T^\dagger)^{-1})$. Hence,

$$\mathcal{R}(T^\dagger) \subset \mathcal{R}(T^\dagger (I + \delta T T^\dagger)^{-1}). \quad (3.6)$$

On the other hand, it is clear that

$$\mathcal{R}(T^\dagger (I + \delta T T^\dagger)^{-1}) \subset \mathcal{R}(T^\dagger). \quad (3.7)$$

So, we have

$$\mathcal{R}(T^\dagger (I + \delta T T^\dagger)^{-1}) = \mathcal{R}(T^\dagger). \quad (3.8)$$

For $x \in \mathcal{N}(T^\dagger)$, we have $(I + \delta T T^\dagger)x = x$, which yields $x = (I + \delta T T^\dagger)^{-1}x$. Hence,

$$T^\dagger (I + \delta T T^\dagger)^{-1}x = T^\dagger x = 0, \quad (3.9)$$

that is, $x \in \mathcal{N}(T^\dagger (I + \delta T T^\dagger)^{-1})$. This implies that

$$\mathcal{N}(T^\dagger) \subset \mathcal{N}(T^\dagger (I + \delta T T^\dagger)^{-1}). \quad (3.10)$$

For $x \in \mathcal{N}(T^\dagger (I + \delta T T^\dagger)^{-1})$, we have $T^\dagger (I + \delta T T^\dagger)^{-1}x = 0$. Let $(I + \delta T T^\dagger)^{-1}x = y$, then $y \in \mathcal{N}(T^\dagger)$, and, hence, $x = (I + \delta T T^\dagger)y = y$. This means

$$\mathcal{N}(T^\dagger (I + \delta T T^\dagger)^{-1}) \subset \mathcal{N}(T^\dagger). \quad (3.11)$$

Consequently,

$$\mathcal{N}(T^\dagger (I + \delta T T^\dagger)^{-1}) = \mathcal{N}(T^\dagger). \quad (3.12)$$

For the sufficiency, we assume that

$$\mathcal{N}(T) \subset \mathcal{N}(\delta T) \quad \text{and} \quad \mathcal{R}(\delta T|_{\mathcal{D}(T)}) \subset \mathcal{R}(T). \quad (3.13)$$

The inclusion $\mathcal{N}(T) \subset \mathcal{N}(\delta T)$ implies $\delta T(I - T^\dagger T) = 0$, which means $\delta T|_{\mathcal{D}(T)} = \delta T T^\dagger T$. The perturbed operator \bar{T} can then be expressed as

$$\bar{T} = (I + \delta T T^\dagger)T. \quad (3.14)$$

As δT is T -bounded and $I + \delta T T^\dagger$ is bijective, we have

$$I + \delta T T^\dagger \in \mathcal{B}(Y), \quad (I + \delta T T^\dagger)^{-1} \in \mathcal{B}(Y). \quad (3.15)$$

The fact that $T \in C(X, Y)$ with a closed range, combined with (3.14) and (3.15), implies that $\bar{T} \in C(X, Y)$ and $\mathcal{R}(\bar{T})$ is closed. From the assumption $\mathcal{R}(\delta T|_{\mathcal{D}(T)}) \subset \mathcal{R}(T)$, we get $\mathcal{R}(\bar{T}) \subset \mathcal{R}(T)$ and $(I - T T^\dagger)\delta T|_{\mathcal{D}(T)} = 0$, which means $\delta T|_{\mathcal{D}(T)} = T T^\dagger \delta T|_{\mathcal{D}(T)}$, and so

$$\bar{T} T^\dagger = T T^\dagger (I + \delta T T^\dagger). \quad (3.16)$$

Moreover, since $I + \delta T T^\dagger$ is surjective and $\mathcal{R}(T) = \mathcal{R}(T T^\dagger)$, we deduce $\mathcal{R}(T) = \mathcal{R}(\bar{T} T^\dagger) \subset \mathcal{R}(\bar{T})$. Thus, we obtain

$$\mathcal{R}(T) = \mathcal{R}(\bar{T}). \quad (3.17)$$

Let $S = T^\dagger (I + \delta T T^\dagger)^{-1}$. It is clear that

$$\mathcal{D}(S) = Y = \mathcal{R}(\bar{T}) \oplus \mathcal{R}(\bar{T})^\perp. \quad (3.18)$$

The relations (3.14) and (3.8) imply $S \bar{T} = T^\dagger T$ and $\mathcal{R}(S) = \mathcal{R}(T^\dagger)$. Hence,

$$\mathcal{R}(S) \subset \mathcal{D}(\bar{T}), \quad S \bar{T} = P_{\mathcal{R}(S)|_{\mathcal{D}(\bar{T})}}. \quad (3.19)$$

Similarly, the relations (3.16) and (3.12) give

$$\bar{T} S = T T^\dagger, \quad \mathcal{N}(S) = \mathcal{N}(T^\dagger). \quad (3.20)$$

The above equations together with (3.17) means

$$\mathcal{N}(S) = \mathcal{R}(\bar{T})^\perp, \quad \bar{T} S = P_{\mathcal{R}(\bar{T})|_{\mathcal{D}(S)}}. \quad (3.21)$$

It follows from (3.19) and (3.21) that

$$S = \bar{T}^\dagger. \quad (3.22)$$

For the necessity, we suppose that $\bar{T} \in C(X, Y)$ and $\bar{T}^\dagger = T^\dagger (I + \delta T T^\dagger)^{-1}$. The relations (3.8) and (3.12) mean $\mathcal{R}(\bar{T}^\dagger) = \mathcal{R}(T^\dagger)$ and $\mathcal{N}(\bar{T}^\dagger) = \mathcal{N}(T^\dagger)$. By Lemma 1(i), we have

$$\mathcal{N}(\bar{T}) = \mathcal{N}(T), \quad \mathcal{R}(\bar{T}) = \mathcal{R}(T). \quad (3.23)$$

The above equations imply $\mathcal{N}(T) \subset \mathcal{N}(\delta T)$ and $\mathcal{R}(\delta T|_{\mathcal{D}(T)}) \subset \mathcal{R}(T)$. The above proof demonstrates the equivalence of (3.4) and (3.5).

Finally, by $\mathcal{R}(\bar{T}) = \mathcal{R}(T)$, we have that $\mathcal{R}(\bar{T})$ is closed.

We now apply Proposition 1 to derive the maximal Tseng generalized inverse of a 2×2 block operator matrix. By viewing the off-diagonal entries of the matrix as a perturbation to the diagonal entries, we obtain the following result.

Theorem 1. *Let $\mathcal{M} = \begin{pmatrix} A & B \\ C & D \end{pmatrix} \in \mathcal{L}(X \times Y)$ be a block operator. The diagonal operators $A \in \mathcal{C}(X)$ and $D \in \mathcal{C}(Y)$ possess bounded maximal Tseng generalized inverses A^\dagger and D^\dagger , respectively. Assume that the off-diagonal operator C is A -bounded and B is D -bounded. Consequently, there exist nonnegative constants a_1, b_1, a_2, b_2 such that*

$$\|Cx\| \leq a_1\|x\| + b_1\|Ax\| \quad \text{for all } x \in \mathcal{D}(A), \quad (3.24)$$

$$\|By\| \leq a_2\|y\| + b_2\|Dy\| \quad \text{for all } y \in \mathcal{D}(D). \quad (3.25)$$

These constants are required to satisfy

$$(a_1\|A^\dagger\| + b_1)(a_2\|D^\dagger\| + b_2) < 1. \quad (3.26)$$

Then, the operator \mathcal{M} is closed and its maximal Tseng generalized inverse is given by

$$\mathcal{M}^\dagger = \begin{pmatrix} A^\dagger(I - BD^\dagger CA^\dagger)^{-1} & -A^\dagger BD^\dagger(I - CA^\dagger BD^\dagger)^{-1} \\ -D^\dagger CA^\dagger(I - BD^\dagger CA^\dagger)^{-1} & D^\dagger(I - CA^\dagger BD^\dagger)^{-1} \end{pmatrix}, \quad (3.27)$$

if, and only if,

$$\mathcal{N}(D) \subset \mathcal{N}(B), \quad \mathcal{N}(A) \subset \mathcal{N}(C), \quad \mathcal{R}(B|_{\mathcal{D}(D)}) \subset \mathcal{R}(A), \quad \mathcal{R}(C|_{\mathcal{D}(A)}) \subset \mathcal{R}(D). \quad (3.28)$$

In this case, the range $\mathcal{R}(\mathcal{M})$ is also closed.

Proof. We denote $\mathcal{M} = T + \delta T$, where $T = \begin{pmatrix} A & 0 \\ 0 & D \end{pmatrix}$ and $\delta T = \begin{pmatrix} 0 & B \\ C & 0 \end{pmatrix}$. Since $A^\dagger \in \mathcal{B}(X)$ and $D^\dagger \in \mathcal{B}(Y)$, we have $T^\dagger = \begin{pmatrix} A^\dagger & 0 \\ 0 & D^\dagger \end{pmatrix} \in \mathcal{B}(X \times Y)$. The A -boundedness of C and the D -boundedness of B together imply that δT is T -bounded. Therefore,

$$I + \delta T T^\dagger = \begin{pmatrix} I & BD^\dagger \\ CA^\dagger & I \end{pmatrix} \in \mathcal{B}(X \times Y). \quad (3.29)$$

The definitions of relative boundedness for C and B yield

$$\|CA^\dagger x\| \leq a_1\|A^\dagger x\| + b_1\|AA^\dagger x\| \quad \text{for } x \in X, \quad (3.30)$$

$$\|BD^\dagger y\| \leq a_2\|D^\dagger y\| + b_2\|DD^\dagger y\| \quad \text{for } y \in Y, \quad (3.31)$$

which implies

$$\|CA^\dagger\| \leq a_1\|A^\dagger\| + b_1, \quad (3.32)$$

$$\|BD^\dagger\| \leq a_2\|D^\dagger\| + b_2. \quad (3.33)$$

It follows from $(a_1\|A^\dagger\| + b_1)(a_2\|D^\dagger\| + b_2) < 1$ that

$$\|CA^\dagger\| \|BD^\dagger\| < 1. \quad (3.34)$$

So both $I - CA^\dagger BD^\dagger \in \mathcal{B}(Y)$ and $I - BD^\dagger CA^\dagger \in \mathcal{B}(X)$ are bijective, which implies that $I + \delta TT^\dagger$ is bijective and

$$(I + \delta TT^\dagger)^{-1} = \begin{pmatrix} (I - BD^\dagger CA^\dagger)^{-1} & -BD^\dagger(I - CA^\dagger BD^\dagger)^{-1} \\ -CA^\dagger(I - BD^\dagger CA^\dagger)^{-1} & (I - CA^\dagger BD^\dagger)^{-1} \end{pmatrix} \in \mathcal{B}(X \times Y). \quad (3.35)$$

According to Proposition 1, we obtain that $\mathcal{M} \in C(X \times Y)$ and $\mathcal{M}^\dagger = T^\dagger(I + \delta TT^\dagger)^{-1}$ if, and only if, $\mathcal{N}(T) \subset \mathcal{N}(\delta T)$ and $\mathcal{R}(\delta T|_{\mathcal{D}(T)}) \subset \mathcal{R}(T)$. Here

$$\begin{aligned} T^\dagger(I + \delta TT^\dagger)^{-1} &= \begin{pmatrix} A^\dagger & 0 \\ 0 & D^\dagger \end{pmatrix} \begin{pmatrix} (I - BD^\dagger CA^\dagger)^{-1} & -BD^\dagger(I - CA^\dagger BD^\dagger)^{-1} \\ -CA^\dagger(I - BD^\dagger CA^\dagger)^{-1} & (I - CA^\dagger BD^\dagger)^{-1} \end{pmatrix} \\ &= \begin{pmatrix} A^\dagger(I - BD^\dagger CA^\dagger)^{-1} & -A^\dagger BD^\dagger(I - CA^\dagger BD^\dagger)^{-1} \\ -D^\dagger CA^\dagger(I - BD^\dagger CA^\dagger)^{-1} & D^\dagger(I - CA^\dagger BD^\dagger)^{-1} \end{pmatrix}. \end{aligned} \quad (3.36)$$

Note that the null spaces and ranges are given by

$$\mathcal{N}(T) = \begin{pmatrix} \mathcal{N}(A) \\ \mathcal{N}(D) \end{pmatrix}, \quad \mathcal{N}(\delta T) = \begin{pmatrix} \mathcal{N}(C) \\ \mathcal{N}(B) \end{pmatrix}, \quad (3.37)$$

$$\mathcal{R}(T) = \begin{pmatrix} \mathcal{R}(A) \\ \mathcal{R}(D) \end{pmatrix}, \quad \mathcal{R}(\delta T|_{\mathcal{D}(T)}) = \begin{pmatrix} \mathcal{R}(B|_{\mathcal{D}(D)}) \\ \mathcal{R}(C|_{\mathcal{D}(A)}) \end{pmatrix}. \quad (3.38)$$

By these expressions, it is clear that $\mathcal{N}(T) \subset \mathcal{N}(\delta T)$ and $\mathcal{R}(\delta T|_{\mathcal{D}(T)}) \subset \mathcal{R}(T)$ if, and only if, (3.28) holds. Consequently, $\mathcal{M} \in C(X \times Y)$, and its inverse is given by (3.27) if, and only if, the conditions in (3.28) hold.

Remark 1. In Theorem 1, we can replace \mathcal{M}^\dagger of the form (3.27) by

$$\mathcal{M}^\dagger = \begin{pmatrix} A^\dagger + A^\dagger BD^\dagger(I - CA^\dagger BD^\dagger)^{-1} CA^\dagger & -A^\dagger BD^\dagger(I - CA^\dagger BD^\dagger)^{-1} \\ -D^\dagger(I - CA^\dagger BD^\dagger)^{-1} CA^\dagger & D^\dagger(I - CA^\dagger BD^\dagger)^{-1} \end{pmatrix} \quad (3.39)$$

or

$$\mathcal{M}^\dagger = \begin{pmatrix} A^\dagger(I - BD^\dagger CA^\dagger)^{-1} & -A^\dagger(I - BD^\dagger CA^\dagger)^{-1} BD^\dagger \\ -D^\dagger CA^\dagger(I - BD^\dagger CA^\dagger)^{-1} & D^\dagger + D^\dagger CA^\dagger(I - BD^\dagger CA^\dagger)^{-1} BD^\dagger \end{pmatrix}. \quad (3.40)$$

Proof. It follows from $(I - CA^\dagger BD^\dagger)CA^\dagger = CA^\dagger(I - BD^\dagger CA^\dagger)$ that

$$(I - CA^\dagger BD^\dagger)^{-1} CA^\dagger = CA^\dagger(I - BD^\dagger CA^\dagger)^{-1}. \quad (3.41)$$

The above equation means

$$\begin{aligned} I + BD^\dagger(I - CA^\dagger BD^\dagger)^{-1} CA^\dagger &= I + BD^\dagger CA^\dagger(I - BD^\dagger CA^\dagger)^{-1} \\ &= I + [I - (I - BD^\dagger CA^\dagger)](I - BD^\dagger CA^\dagger)^{-1} \\ &= (I - BD^\dagger CA^\dagger)^{-1}. \end{aligned} \quad (3.42)$$

By (3.41) and (3.42), we obtain that (3.27) is equivalent to (3.39). Similarly, the equivalence of (3.27) and (3.40) follows from

$$(I - BD^\dagger CA^\dagger)BD^\dagger = BD^\dagger(I - CA^\dagger BD^\dagger). \quad (3.43)$$

To further reveal the internal structure of the maximal Tseng generalized inverse \mathcal{M}^\dagger , we present it in the Banachiewicz-Schur form. This formulation is fundamental in block operator theory because it breaks down the problem of inverting the entire operator into inversions of its diagonal blocks and the corresponding generalized Schur complements.

Corollary 1. Let $\mathcal{M} = \begin{pmatrix} A & B \\ C & D \end{pmatrix} \in \mathcal{L}(X \times Y)$, and $A \in C(X)$ and $D \in C(Y)$ with the maximal Tseng generalized inverses $A^\dagger \in \mathcal{B}(X)$ and $D^\dagger \in \mathcal{B}(Y)$, respectively. Assume that C is A -bounded and B is D -bounded, i.e.,

$$\|Cx\| \leq a_1\|x\| + b_1\|Ax\|, \quad x \in \mathcal{D}(A), \quad (3.44)$$

$$\|By\| \leq a_2\|y\| + b_2\|Dy\|, \quad y \in \mathcal{D}(D), \quad (3.45)$$

where $a_1, b_1, a_2, b_2 \in \mathbb{R}^+$ satisfy $(a_1\|A^\dagger\| + b_1)(a_2\|D^\dagger\| + b_2) < 1$. If (3.28) holds, then $\mathcal{M} \in C(X \times Y)$ and

$$\begin{aligned} \mathcal{M}^\dagger &= \begin{pmatrix} A^\dagger + A^\dagger B(D - CA^\dagger B)^\dagger CA^\dagger & -A^\dagger B(D - CA^\dagger B)^\dagger \\ -(D - CA^\dagger B)^\dagger CA^\dagger & (D - CA^\dagger B)^\dagger \end{pmatrix} \\ &= \begin{pmatrix} (A - BD^\dagger C)^\dagger & -(A - BD^\dagger C)^\dagger BD^\dagger \\ -D^\dagger C(A - BD^\dagger C)^\dagger & D^\dagger + D^\dagger C(A - BD^\dagger C)^\dagger BD^\dagger \end{pmatrix}. \end{aligned} \quad (3.46)$$

In this case, $\mathcal{R}(\mathcal{M})$ is closed.

Proof. It follows from Theorem 1 and Remark 1 that $\mathcal{M} \in C(X \times Y)$ and \mathcal{M}^\dagger is an operator matrix of the form (3.39) or (3.40). To complete the proof, it suffices to prove

$$(D - CA^\dagger B)^\dagger = D^\dagger(I - CA^\dagger BD^\dagger)^{-1}, \quad (3.47)$$

$$(A - BD^\dagger C)^\dagger = A^\dagger(I - BD^\dagger CA^\dagger)^{-1}. \quad (3.48)$$

The identity (3.47) is a direct consequence of Proposition 1 applied to the operator $D - CA^\dagger B$. The operator $CA^\dagger B$ is D -bounded and $I - CA^\dagger BD^\dagger$ is bijective by the assumptions of the corollary. Furthermore, the relations $\mathcal{N}(D) \subset \mathcal{N}(B)$ and $\mathcal{R}(C|_{\mathcal{D}(A)}) \subset \mathcal{R}(D)$ imply

$$\mathcal{N}(D) \subset \mathcal{N}(CA^\dagger B) \quad \text{and} \quad \mathcal{R}(CA^\dagger B|_{\mathcal{D}(D)}) \subset \mathcal{R}(D). \quad (3.49)$$

Hence, Proposition 1 is applicable and yields

$$(D - CA^\dagger B)^\dagger = D^\dagger(I - CA^\dagger BD^\dagger)^{-1}. \quad (3.50)$$

We now turn to the identity (3.48) and apply Proposition 1 to the operator $A - BD^\dagger C$. The corollary's assumptions provide that the operator $BD^\dagger C$ is A -bounded and $I - BD^\dagger CA^\dagger$ is bijective. The relations $\mathcal{N}(A) \subset \mathcal{N}(C)$ and $\mathcal{R}(B|_{\mathcal{D}(D)}) \subset \mathcal{R}(A)$ follow

$$\mathcal{N}(A) \subset \mathcal{N}(BD^\dagger C) \quad \text{and} \quad \mathcal{R}(BD^\dagger C|_{\mathcal{D}(A)}) \subset \mathcal{R}(A). \quad (3.51)$$

Consequently, we obtain (3.48)

$$(A - BD^\dagger C)^\dagger = A^\dagger(I - BD^\dagger CA^\dagger)^{-1}. \quad (3.52)$$

When the operator \mathcal{M} is bounded and block upper-triangular (i.e., $C = 0$), Theorem 1 naturally reduces to the following well-known result for the Moore-Penrose inverse, which can be found in [33].

Corollary 2. *Let $\mathcal{M} = \begin{pmatrix} A & B \\ 0 & D \end{pmatrix} \in \mathcal{B}(X \times Y)$, $\mathcal{R}(A)$ and $\mathcal{R}(D)$ be closed. Then, $\mathcal{M}^\dagger = \begin{pmatrix} A^\dagger & -A^\dagger B D^\dagger \\ 0 & D^\dagger \end{pmatrix}$ if, and only if, $\mathcal{R}(B) \subset \mathcal{R}(A)$ and $\mathcal{N}(D) \subset \mathcal{N}(B)$. In this case, $\mathcal{R}(\mathcal{M})$ is closed and \mathcal{M}^\dagger is the Moore-Penrose inverse of \mathcal{M} .*

Classical block inversion methods, such as those based on the Schur complement, fundamentally rely on the invertibility of the diagonal blocks. However, structural singularities can arise from specific physical conditions of the scattering experiment rendering such methods inapplicable. We now present an example to illustrate the necessity of our generalized inverse framework.

We consider a one-dimensional inverse problem discretized on a minimal grid of two points. The structure of the operators \mathcal{J}_ρ and \mathcal{J}_κ is derived from the Lippmann-Schwinger integral equation. As discussed previously, the distinct mathematical forms of the density and bulk modulus terms lead to different sensitivities to experimental parameters. In a scenario characteristic of a low-frequency experiment, the measurement system is unable to resolve the individual contributions of the density contrasts. This physical limit results in the integral operator being discretized as

$$\mathcal{J}_\rho = \begin{pmatrix} 1 & 1 \\ 1 & 1 \end{pmatrix} \quad \text{and} \quad \mathcal{J}_\kappa = \begin{pmatrix} 1 & 0 \\ 0 & 1 \end{pmatrix}. \quad (3.53)$$

The distinct mathematical forms of the density and bulk modulus terms lead to different sensitivities to experimental parameters. To reveal the impact of the physical cross-coupling strength on the inversion stability, we introduce a parameter $0 < \gamma < 1$ to represent this strength. Consequently, the normal operator $M = \mathcal{J}^* \mathcal{J}$ has the block structure defined in (2.17), where the diagonal blocks A , D and the off-diagonal coupling blocks B , C are given explicitly by

$$A = \mathcal{J}_\rho^T \mathcal{J}_\rho = \begin{pmatrix} 2 & 2 \\ 2 & 2 \end{pmatrix}, \quad B = \gamma \mathcal{J}_\rho^T \mathcal{J}_\kappa = \gamma \begin{pmatrix} 1 & 1 \\ 1 & 1 \end{pmatrix}, \quad (3.54)$$

$$C = \gamma \mathcal{J}_\kappa^T \mathcal{J}_\rho = \gamma \begin{pmatrix} 1 & 1 \\ 1 & 1 \end{pmatrix}, \quad D = \mathcal{J}_\kappa^T \mathcal{J}_\kappa = \begin{pmatrix} 1 & 0 \\ 0 & 1 \end{pmatrix}. \quad (3.55)$$

For clarity in this example, we explicitly include the scaling factor γ in the definitions of the off-diagonal blocks B and C .

The diagonal block A is singular, as $\det(A) = 0$. The nonexistence of A^{-1} therefore precludes the application of any classical inversion method based on the Schur complement, irrespective of the coupling strength γ . However, our method remains applicable. To confirm this, we sequentially verify the conditions of Theorem 1.

- i. **Null Space and Range Conditions:** The key inclusions $\mathcal{N}(A) \subset \mathcal{N}(C)$ and $\mathcal{R}(B) \subset \mathcal{R}(A)$ hold for any $0 < \gamma < 1$, since the null and range spaces of B and C are identical to those of A . The conditions involving the invertible operator D , namely, $\mathcal{N}(D) \subset \mathcal{N}(B)$ and $\mathcal{R}(C) \subset \mathcal{R}(D)$, are satisfied trivially.
- ii. **Boundedness Condition:** For the finite-dimensional case, the relative boundedness condition of Theorem 1 simplifies to $\|A^\dagger\| \|B\| \|C\| \|D^\dagger\| < 1$. A direct calculation yields $\|A^\dagger\| = 1/4$, $\|B\| = \|C\| = 2\gamma$, and $\|D^\dagger\| = 1$. For $0 < \gamma < 1$, the product is

$$(1/4) \cdot (2\gamma) \cdot (2\gamma) \cdot 1 = \gamma^2 < 1. \quad (3.56)$$

Thus, the strict inequality is satisfied.

Since all prerequisites of Theorem 1 are met, the existence of a well-defined generalized inverse \mathcal{M}^\dagger is guaranteed, providing a rigorous pathway to a solution. This example illustrates that our generalized inverse framework is not merely an abstract reformulation but an essential and powerful tool, capable of providing analytical solutions to structurally singular inverse problems that are intractable for classical approaches.

4. Structure and stability of the regularized solution

It is well known that the inverse problem is fundamentally ill-posed. The minimum-norm least-squares solution $\mathbf{m}^\dagger = \mathcal{M}^\dagger \mathcal{J}^* u_{\text{obs}}$ of (2.18) is notoriously sensitive to noise. The mathematical origin of this instability lies in the spectral properties of the normal operator $\mathcal{M} = \mathcal{J}^* \mathcal{J}$. Since the forward operator \mathcal{J} is a compact integral operator, \mathcal{M} is also compact. Consequently, its spectrum consists of a sequence of nonnegative eigenvalues that accumulate at zero. This lack of a positive lower bound on the spectrum makes its generalized inverse \mathcal{M}^\dagger an unbounded operator, which leads to the severe amplification of measurement noise.

To obtain a stable solution, we construct a well-posed approximation of the original problem. The ill-posedness of operator \mathcal{M} stems from the presence of zero or near-zero eigenvalues. A straightforward regularization method is the spectral shift, which replaces \mathcal{M} with a modified operator whose spectrum is uniformly bounded away from zero. For a parameter $\alpha > 0$, this is achieved by constructing the operator

$$\mathcal{M}_\alpha := \mathcal{M} + \alpha I. \quad (4.1)$$

This operation is known as Tikhonov regularization. It is a classical result of Tikhonov regularization theory that as $\alpha \rightarrow 0^+$, the regularized solution \mathbf{m}_α converges to the minimum-norm least-squares solution \mathbf{m}^\dagger [1].

This section is devoted to a rigorous analysis of the Tikhonov-regularized solution \mathbf{m}_α . We begin by showing that the regularized operator \mathcal{M}_α satisfies the hypotheses of the block operator framework. Subsequently, we derive the explicit form of the solution and decompose its structure to characterize the relationship between parameter coupling and regularization. Finally, based on this structural analysis, we derive an explicit stability bound that quantifies the sensitivity of the solution to data errors.

4.1. Regularization and applicability of Theorem 1

Following the motivation above, we consider the Tikhonov-regularized system

$$\mathcal{M}_\alpha \mathbf{m}_\alpha = \mathcal{J}^* u_{\text{obs}}. \quad (4.2)$$

To analyze the structure of the operator $(\mathcal{M}_\alpha)^{-1}$, we first verify that the regularized operator \mathcal{M}_α satisfies the necessary conditions of Theorem 1.

Lemma 2. *Let $\mathcal{M}_\alpha = \begin{pmatrix} A_\alpha & B \\ C & D_\alpha \end{pmatrix}$ with $A_\alpha = A + \alpha I$ and $D_\alpha = D + \alpha I$, where A, B, C, D are defined as in (2.17). If the regularization parameter $\alpha > \sqrt{\|B\| \|C\|}$, then \mathcal{M}_α satisfies all conditions of Theorem 1. Specifically,*

(i) The operators A_α and D_α are bounded, invertible operators, and their maximal Tseng generalized inverses are their ordinary inverses, i.e.,

$$A_\alpha^\dagger = A_\alpha^{-1} \quad \text{and} \quad D_\alpha^\dagger = D_\alpha^{-1}. \quad (4.3)$$

(ii) The operator C is A_α -bounded and B is D_α -bounded.

(iii) The inequality $\|C\| \|A_\alpha^{-1}\| \|B\| \|D_\alpha^{-1}\| < 1$ holds.

(iv) The null space and range of A_α , D_α , B , and C satisfy

$$\mathcal{N}(A_\alpha) \subset \mathcal{N}(C), \quad \mathcal{N}(D_\alpha) \subset \mathcal{N}(B), \quad (4.4)$$

and

$$\mathcal{R}(B) \subset \mathcal{R}(A_\alpha), \quad \mathcal{R}(C) \subset \mathcal{R}(D_\alpha). \quad (4.5)$$

Proof. (i) The operators $A = \mathcal{J}_\rho^* \mathcal{J}_\rho$ and $D = \mathcal{J}_\kappa^* \mathcal{J}_\kappa$ satisfy

$$\langle A m_\rho, m_\rho \rangle = \|\mathcal{J}_\rho m_\rho\|^2 \geq 0 \quad \text{and} \quad \langle D m_\kappa, m_\kappa \rangle = \|\mathcal{J}_\kappa m_\kappa\|^2 \geq 0 \quad (4.6)$$

for any $m_\rho, m_\kappa \in L^2(\Omega)$, and are thus positive semi-definite. It follows that for $\alpha > 0$ and any nonzero $m_\rho, m_\kappa \in L^2(\Omega)$, we obtain

$$\langle A_\alpha m_\rho, m_\rho \rangle = \|\mathcal{J}_\rho m_\rho\|^2 + \alpha \|m_\rho\|^2 > 0, \quad (4.7)$$

$$\langle D_\alpha m_\kappa, m_\kappa \rangle = \|\mathcal{J}_\kappa m_\kappa\|^2 + \alpha \|m_\kappa\|^2 > 0. \quad (4.8)$$

Hence, the regularized operators $A_\alpha = A + \alpha I$ and $D_\alpha = D + \alpha I$ are consequently strictly positive definite. As bounded, self-adjoint, strictly positive definite operators on a Hilbert space, both A_α and D_α are invertible with bounded inverses. For invertible operators, the maximal Tseng generalized inverse coincides with the ordinary inverse.

(ii) Since the integral operators \mathcal{J}_ρ and \mathcal{J}_κ are bounded, the operators A, B, C, D are bounded on $L^2(\Omega)$. Consequently, the relative boundedness conditions required by Theorem 1 are trivially satisfied. We can choose the constants in the inequalities (3.24) and (3.25) as

$$a_1 = \|C\|, \quad b_1 = 0, \quad \text{and} \quad a_2 = \|B\|, \quad b_2 = 0. \quad (4.9)$$

With these choices, the condition $\|Cx\| \leq \|C\| \|x\|$ trivially holds for C being A_α -bounded, and similarly for B being D_α -bounded.

(iii) Since A is a positive semi-definite, self-adjoint operator, its spectrum satisfies $\sigma(A) \subset [0, \infty)$. The spectral mapping theorem implies that $\sigma(A + \alpha I) = \{\lambda + \alpha \mid \lambda \in \sigma(A)\}$, and thus $\sigma(A + \alpha I) \subset [\alpha, \infty)$. For an invertible self-adjoint operator T , the norm of its inverse is given by $\|T^{-1}\| = 1 / \inf\{|\mu| \mid \mu \in \sigma(T)\}$. Applying this to $A + \alpha I$, we obtain

$$\|(A + \alpha I)^{-1}\| = \frac{1}{\inf\{|\mu| \mid \mu \in \sigma(A + \alpha I)\}} = \frac{1}{\inf \sigma(A) + \alpha} \leq \frac{1}{\alpha}. \quad (4.10)$$

A similar argument yields the bound $\|(D + \alpha I)^{-1}\| \leq 1/\alpha$. Therefore, if

$$\alpha > \sqrt{\|B\| \|C\|}, \quad (4.11)$$

then $\|C\| \|A_\alpha^{-1}\| \|B\| \|D_\alpha^{-1}\| < 1$. With the constants from (ii), $(a_1 \|A_\alpha^{-1}\| + b_1)(a_2 \|D_\alpha^{-1}\| + b_2) < 1$ holds.

(iv) The invertibility of A_α and D_α means

$$\mathcal{N}(A_\alpha) = \mathcal{N}(D_\alpha) = \{0\} \quad \text{and} \quad \mathcal{R}(A_\alpha) = \mathcal{R}(D_\alpha) = L^2(\Omega). \quad (4.12)$$

It is clear that

$$\mathcal{N}(A_\alpha) \subset \mathcal{N}(C), \quad \mathcal{N}(D_\alpha) \subset \mathcal{N}(B), \quad (4.13)$$

and

$$\mathcal{R}(B) \subset \mathcal{R}(A_\alpha), \quad \mathcal{R}(C) \subset \mathcal{R}(D_\alpha). \quad (4.14)$$

This completes the proof.

The verification in Lemma 2 confirms the applicability of our operator-theoretic method to the regularized problem. The main contribution of this method is its ability to deconstruct the operator $(\mathcal{M}_\alpha)^{-1}$. This deconstruction is rooted in the spectral properties of the block operators A_α, B, C , and D_α . It allows for a quantitative analysis of parameter coupling by linking it directly to operator norm and spectrum.

4.2. Explicit form and structure of the regularized solution

Since \mathcal{M}_α satisfies the conditions of Theorem 1 and is invertible, we can apply Theorem 1 to obtain the explicit form of its inverse $(\mathcal{M}_\alpha)^{-1}$.

Theorem 2. Assume the regularization parameter $\alpha > \sqrt{\|B\| \|C\|}$. Then, the inverse of the regularized operator \mathcal{M}_α is given by

$$(\mathcal{M}_\alpha)^{-1} = \begin{pmatrix} A_\alpha^{-1}(I - S_1)^{-1} & -A_\alpha^{-1}BD_\alpha^{-1}(I - S_2)^{-1} \\ -D_\alpha^{-1}CA_\alpha^{-1}(I - S_1)^{-1} & D_\alpha^{-1}(I - S_2)^{-1} \end{pmatrix}, \quad (4.15)$$

where the operators S_1 and S_2 are defined as

$$S_1 = BD_\alpha^{-1}CA_\alpha^{-1} \quad \text{and} \quad S_2 = CA_\alpha^{-1}BD_\alpha^{-1}. \quad (4.16)$$

Proof. It follows from Lemma 2 and Theorem 1 that the representation (4.15) is valid provided that the factors $(I - S_1)$ and $(I - S_2)$ are invertible. Using the bounds $\|A_\alpha^{-1}\| \leq \alpha^{-1}$ and $\|D_\alpha^{-1}\| \leq \alpha^{-1}$, we obtain

$$\|S_1\| \leq \|B\| \|D_\alpha^{-1}\| \|C\| \|A_\alpha^{-1}\| \leq \frac{\|B\| \|C\|}{\alpha^2}. \quad (4.17)$$

The condition $\alpha > \sqrt{\|B\| \|C\|}$ implies $\|S_1\| < 1$. Analogous arguments yield $\|S_2\| < 1$. Consequently, both $I - S_1$ and $I - S_2$ are invertible, which completes the proof.

With the explicit form of the solution operator $(\mathcal{M}_\alpha)^{-1}$ established in (4.15), we now analyze the detailed structure of the regularized solution $\mathbf{m}_\alpha = (\mathcal{M}_\alpha)^{-1} \mathcal{J}^* u_{\text{obs}}$. The following corollary presents the individual components of the solution vector.

Corollary 3. Assume the regularization parameter $\alpha > \sqrt{\|B\| \|C\|}$. Let $\mathbf{m}_\alpha = (m_{\rho,\alpha}, m_{\kappa,\alpha})^\top$ be the solution to the regularized system (4.2). Then, the components $m_{\rho,\alpha}$ and $m_{\kappa,\alpha}$ are given by

$$m_{\rho,\alpha} = A_\alpha^{-1}(I - S_1)^{-1}(\mathcal{J}_\rho^* u_{\text{obs}}) - A_\alpha^{-1}BD_\alpha^{-1}(I - S_2)^{-1}(\mathcal{J}_\kappa^* u_{\text{obs}}), \quad (4.18)$$

$$m_{\kappa,\alpha} = D_\alpha^{-1}(I - S_2)^{-1}(\mathcal{J}_\kappa^* u_{\text{obs}}) - D_\alpha^{-1}CA_\alpha^{-1}(I - S_1)^{-1}(\mathcal{J}_\rho^* u_{\text{obs}}). \quad (4.19)$$

The explicit forms in (4.18) and (4.19) decompose each solution component into two distinct terms. We only consider $m_{\rho,\alpha}$, since the case of $m_{\kappa,\alpha}$ is similar. The first term $A_\alpha^{-1}(I - BD_\alpha^{-1}CA_\alpha^{-1})^{-1}(\mathcal{J}_\rho^*u_{\text{obs}})$ is associated with the data term $\mathcal{J}_\rho^*u_{\text{obs}}$. We expand the inverse operator $(I - BD_\alpha^{-1}CA_\alpha^{-1})^{-1}$ using the Neumann series

$$(I - BD_\alpha^{-1}CA_\alpha^{-1})^{-1} = \sum_{n=0}^{\infty} (BD_\alpha^{-1}CA_\alpha^{-1})^n, \quad (4.20)$$

which converges since $\|BD_\alpha^{-1}CA_\alpha^{-1}\| < 1$. The leading component of this expansion yields the term $A_\alpha^{-1}(\mathcal{J}_\rho^*u_{\text{obs}})$. The remaining higher-order components all involve the off-diagonal operators B and C . The second term explicitly contains the off-diagonal operator B as a multiplicative factor and is driven by the data term $\mathcal{J}_\kappa^*u_{\text{obs}}$. Consequently, every component resulting from the expansion of this term involves at least one off-diagonal operator. Thus, the leading term of the complete solution for $m_{\rho,\alpha}$ is $A_\alpha^{-1}(\mathcal{J}_\rho^*u_{\text{obs}})$. This is the only component of the solution that involves exclusively the diagonal operators. All subsequent terms, which form an infinite series, necessarily involve the off-diagonal coupling operators B or C .

The regularization parameter α governs the balance between the leading, diagonal-only term and the subsequent series of terms involving off-diagonal operators. Its primary role is to control the convergence of the Neumann series. As $\alpha \rightarrow \infty$, the norms of all terms containing the off-diagonal operators B or C tend to zero. This is because every such term contains at least one factor of A_α^{-1} or D_α^{-1} , whose norms are bounded by $1/\alpha$. Consequently, the infinite series of non-diagonal terms vanishes, and the solution $(m_{\rho,\alpha}, m_{\kappa,\alpha})$ converges to $(A_\alpha^{-1}\mathcal{J}_\rho^*u_{\text{obs}}, D_\alpha^{-1}\mathcal{J}_\kappa^*u_{\text{obs}})$. Conversely, as α decreases toward its lower bound $\sqrt{\|B\|\|C\|}$, the upper bound for the norm of the operator $BD_\alpha^{-1}CA_\alpha^{-1}$ approaches 1. According to the Neumann series expansion (4.20), this slower convergence rate results in an amplification of the higher-order terms.

4.3. Stability analysis of the regularized solution

We now analyze the stability of the Tikhonov-regularized solution with respect to perturbations in the data. The solution \mathbf{m}_α is obtained by minimizing the functional $\|\mathcal{J}\mathbf{m} - u_{\text{obs}}\|^2 + \alpha^2\|\mathbf{m}\|^2$. In any practical scenario, the observed data u_{obs} will not perfectly match any model prediction $\mathcal{J}\mathbf{m}$, due to a combination of measurement noise and the inherent limitations of the linearized forward problem.

Let u_{exact} and u_{obs} be the exact and observed data, respectively. We denote the Tikhonov-regularized solutions computed from the exact and observed data as $\mathbf{m}_{\alpha,\text{exact}}$ and $\mathbf{m}_{\alpha,\text{obs}}$, respectively. Let data error be denoted as $\delta u = u_{\text{obs}} - u_{\text{exact}}$. We derive an explicit bound for the error $\delta\mathbf{m} = \mathbf{m}_{\alpha,\text{obs}} - \mathbf{m}_{\alpha,\text{exact}}$ in terms of δu .

Theorem 3. *Under the conditions of Lemma 2, for any regularization parameter $\alpha > \sqrt{\|B\|\|C\|}$, the bound of $\delta\mathbf{m}$ is given by*

$$\|\delta\mathbf{m}\| \leq \frac{\sqrt{2\alpha^2 + \|B\|^2 + \|C\|^2}}{\alpha^2 - \|B\|\|C\|} \|\mathcal{J}\|\|\delta u\|. \quad (4.21)$$

Proof. From the definition of the Tikhonov-regularized solution, we have

$$\mathbf{m}_{\alpha,\text{obs}} = (\mathcal{M}_\alpha)^{-1} \mathcal{J}^* u_{\text{obs}}, \quad (4.22)$$

$$\mathbf{m}_{\alpha,\text{exact}} = (\mathcal{M}_\alpha)^{-1} \mathcal{J}^* u_{\text{exact}}. \quad (4.23)$$

Subtracting these two equations yields

$$\delta \mathbf{m} = (\mathcal{M}_\alpha)^{-1} \mathcal{J}^*(u_{\text{obs}} - u_{\text{exact}}) = (\mathcal{M}_\alpha)^{-1} \mathcal{J}^* \delta u. \quad (4.24)$$

where the form of $(\mathcal{M}_\alpha)^{-1}$ is given by (4.15). Taking the norm of both sides of (4.24), we obtain

$$\|\delta \mathbf{m}\| \leq \|(\mathcal{M}_\alpha)^{-1}\| \|\mathcal{J}\| \|\delta u\|. \quad (4.25)$$

The core of the proof is to derive an explicit upper bound for the operator norm $\|(\mathcal{M}_\alpha)^{-1}\|$. To simplify the notation, we denote the four block components of \mathcal{M}_α^{-1} by T_{ij} for $i, j \in \{1, 2\}$. A simple calculation yields

$$\|(\mathcal{M}_\alpha)^{-1}\| \leq \sqrt{\|T_{11}\|^2 + \|T_{12}\|^2 + \|T_{21}\|^2 + \|T_{22}\|^2}. \quad (4.26)$$

Recalling the definitions of S_1 and S_2 from Theorem 2, it follows from $\alpha > \sqrt{\|B\|\|C\|}$ that

$$\|S_1\| \leq \|B\|\|D_\alpha^{-1}\|\|C\|\|A_\alpha^{-1}\| \leq \frac{\|B\|\|C\|}{\alpha^2} < 1, \quad (4.27)$$

$$\|S_2\| \leq \|C\|\|A_\alpha^{-1}\|\|B\|\|D_\alpha^{-1}\| \leq \frac{\|B\|\|C\|}{\alpha^2} < 1. \quad (4.28)$$

Denote $\gamma^2 := \|B\|\|C\|$. The Neumann series estimate for the inverse operator implies

$$\|(I - S_1)^{-1}\| \leq \frac{1}{1 - \|S_1\|} \leq \frac{1}{1 - \gamma^2/\alpha^2} = \frac{\alpha^2}{\alpha^2 - \gamma^2}, \quad (4.29)$$

and an identical bound holds for $\|(I - S_2)^{-1}\|$. The norms of the block components T_{ij} are bounded as

$$\|T_{11}\| = \|A_\alpha^{-1}(I - S_1)^{-1}\| \leq \|A_\alpha^{-1}\| \|(I - S_1)^{-1}\| \leq \frac{1}{\alpha} \frac{\alpha^2}{\alpha^2 - \gamma^2} = \frac{\alpha}{\alpha^2 - \gamma^2}, \quad (4.30)$$

$$\|T_{12}\| \leq \|A_\alpha^{-1}\|\|B\|\|(I - S_2)^{-1}\|\|D_\alpha^{-1}\| \leq \frac{1}{\alpha} \|B\| \frac{\alpha^2}{\alpha^2 - \gamma^2} \frac{1}{\alpha} = \frac{\|B\|}{\alpha^2 - \gamma^2}, \quad (4.31)$$

$$\|T_{21}\| \leq \|D_\alpha^{-1}\|\|C\|\|(I - S_1)^{-1}\|\|A_\alpha^{-1}\| \leq \frac{\|C\|}{\alpha^2 - \gamma^2}, \quad (4.32)$$

$$\|T_{22}\| \leq \|D_\alpha^{-1}\|\|(I - S_2)^{-1}\| \leq \frac{\alpha}{\alpha^2 - \gamma^2}. \quad (4.33)$$

Substituting (4.30)–(4.33) into (4.26) and noting the common denominator $(\alpha^2 - \gamma^2)^2$, we obtain

$$\|(\mathcal{M}_\alpha)^{-1}\|^2 \leq \frac{\alpha^2 + \|B\|^2 + \|C\|^2 + \alpha^2}{(\alpha^2 - \gamma^2)^2} = \frac{2\alpha^2 + \|B\|^2 + \|C\|^2}{(\alpha^2 - \gamma^2)^2}. \quad (4.34)$$

Taking the square root and recalling that $\gamma^2 = \|B\|\|C\|$, we have

$$\|(\mathcal{M}_\alpha)^{-1}\| \leq \frac{\sqrt{2\alpha^2 + \|B\|^2 + \|C\|^2}}{\alpha^2 - \gamma^2}. \quad (4.35)$$

Combining this with (4.25) yields the final stability estimate (4.21).

Remark 2. While a small regularization parameter α is generally desired for the solution to converge to the generalized solution \mathbf{m}^\dagger , our stability analysis reveals a critical constraint imposed by parameter coupling. If $B = C = 0$, the error bound from Theorem 3 is governed by the factor $\sqrt{2}/\alpha$. However, in the case where B and C are nonzero, the bound is determined by

$$\frac{\sqrt{2\alpha^2 + \|B\|^2 + \|C\|^2}}{\alpha^2 - \|B\|\|C\|}. \quad (4.36)$$

This factor is evidently larger than the decoupled bound. As α approaches the threshold $\sqrt{\|B\|\|C\|}$ from above, the error bound grows without bound. This singular behavior demonstrates that the coupling strength imposes a fundamental limit on how close the regularized solution can approach the generalized solution in a stable way.

The practical implications of the stability bound in Theorem 3 warrant a brief discussion. While estimating the norms of continuous operators is challenging, any numerical solution relies on a discretized model where the operators become matrices. For such systems, the norms $\|B\|$ and $\|C\|$ can be computed or estimated, allowing α_{crit} to serve as a tangible guideline for selecting a stable regularization parameter. To conclude our analysis, we present a numerical experiment that corroborates the theoretical findings, particularly focusing on the role of the coupling-induced stability bound.

Example 1. Consider a discretized system built from two identical 5×5 ill-posed Toeplitz matrices, \mathcal{J}_ρ and \mathcal{J}_κ , with entries $(\mathcal{J}_\rho)_{ij} = \exp(-2|i - j|)$. Based on the stability condition in Theorem 1, we set the coupling strength to be $\gamma = 0.05$. This parameterization results in a theoretical lower bound for regularization, $\alpha_{\text{crit}} \approx 0.0791$, which serves as the benchmark for our stability test. The reconstruction performance is evaluated using the relative total error \mathcal{E} , defined as

$$\mathcal{E} := \frac{\|m_\alpha - m_{\text{true}}\|}{\|m_{\text{true}}\|}, \quad (4.37)$$

where m_α is the regularized solution for a given α , and m_{true} is the ground-truth vector.

Figure 1 numerically validates our stability analysis, highlighting the relationship between the empirical optimal parameter α_{opt} and the theoretical threshold α_{crit} . Our stability estimate (Theorem 3) is a worst-case upper bound derived from norm inequalities, which explains why α_{opt} may reside slightly in the theoretically unstable region ($\alpha < \alpha_{\text{crit}}$) at low noise levels, as the actual noise is unlikely to trigger the worst-case amplification.

However, as noise increases, the error amplification dominates, forcing α_{opt} into the conservatively stable region ($\alpha > \alpha_{\text{crit}}$). This confirms that α_{crit} serves as a critical stability landmark. For any nontrivial noise, choosing a parameter safely above this threshold is essential for a robust inversion, effectively guarding against the worst-case instabilities predicted by our theory.

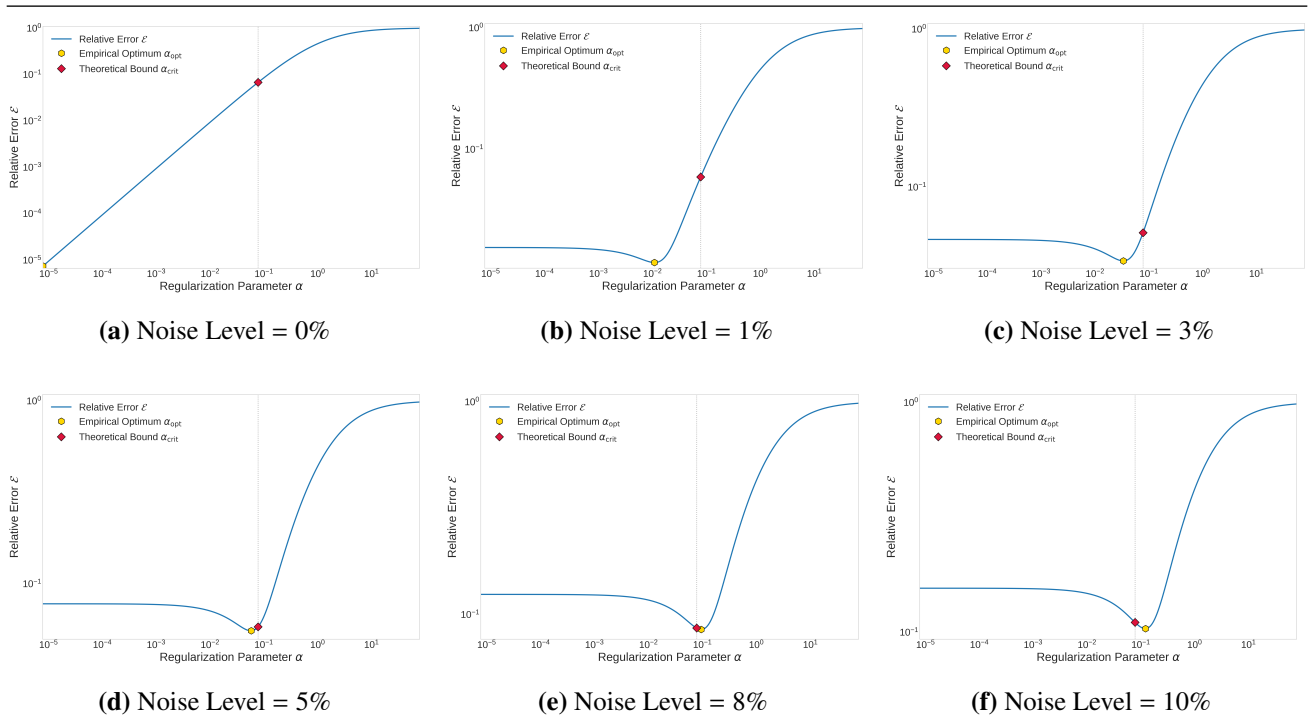


Figure 1. The stability estimate under varying noise levels.

5. Conclusions

In this paper, we employed the maximal Tseng generalized inverse to investigate the two-parameter acoustic inverse scattering problem. This approach provides an explicit analytical solution even for systems with singular diagonal blocks where traditional methods fail. Our analysis of the Tikhonov-regularized problem revealed a fundamental stability threshold α_{crit} , determined by the parameter coupling strength. Our key contribution is the identification and quantification of a fundamental limit in the Tikhonov regularization of linearized multiparameter problems. We derived an explicit bound for the regularization parameter α_{crit} , demonstrating that it is dictated by parameter cross-talk and serves as a hard threshold for stable inversion. The numerical results validate α_{crit} as a critical stability landmark. While precisely computing this bound in practice can be challenging, its existence reveals a hard limit on reconstruction fidelity imposed by the system's physics. This insight is of significant consequence for applications in medical imaging and geophysics, as the inherent limitation cannot be circumvented merely by enhancing data quality.

In the future, we plan to extend our analysis beyond the Born approximation to full nonlinear problems. Additionally, we hope to investigate the applicability of our operator-theoretic approach to similar multiparameter challenges in electromagnetics and elastodynamics.

Use of AI tools declaration

The authors declare they have not used Artificial Intelligence (AI) tools in the creation of this article.

Acknowledgments

The first author is supported by the Natural Science Foundation of Inner Mongolia (No. 2025QN01009), the Research Center for Regional Digital Economy and Digital Governance, Inner Mongolia University of Finance and Economics (No. szzl202532) and the Scientific Research Fund of Inner Mongolia University of Finance and Economics (No. NCXKY25035). The second author is supported by the Shenzhen Sci-Tech Fund (No. RCJC20200714114556020) and the Guangdong Basic and Applied Research Fund (No. 2023B1515250005). The third author is supported by the National Natural Science Foundation of China (NSFC) under grants 12501584 and 12571452, and the China Postdoctoral Science Foundation under grant GZC20252762.

Conflict of interest

The authors declare there are no conflicts of interest.

References

1. D. Colton, R. Kress, *Inverse Acoustic and Electromagnetic Scattering Theory*, Springer, Cham, 2019. <https://doi.org/10.1007/978-3-030-30351-8>.
2. K. Ito, B. Jin, *Inverse Problems, Tikhonov Theory and Algorithms*, World Scientific, Hackensack, 2015. <https://doi.org/10.1142/9120>
3. G. Bao, P. Li, *Maxwell's Equations in Periodic Structures*, Springer, Singapore, 2022. <https://doi.org/10.1007/978-981-16-0061-6>
4. A. C. Kak, M. Slaney, *Principles of Computerized Tomographic Imaging*, SIAM, Philadelphia, 2001. <https://doi.org/10.1137/1.9780898719277>
5. T. Hohage, Logarithmic convergence rates of the iteratively regularized Gauss-Newton method for an inverse potential and an inverse scattering problem, *Inverse Probl.*, **13** (1997), 1279–1299. <https://doi.org/10.1088/0266-5611/13/5/012>
6. W. C. Chew, Y. M. Wang, Reconstruction of two-dimensional permittivity distribution using the distorted Born iterative method, *IEEE Trans. Med. Imaging*, **9** (1990), 218–225. <https://doi.org/10.1109/42.56334>
7. A. N. Tikhonov, V. Y. Arsenin, *Solutions of Ill-Posed Problems*, John Wiley & Sons, New York, 1977. <https://doi.org/10.1137/1021044>
8. H. W. Engl, M. Hanke, A. Neubauer, *Regularization of Inverse Problems*, Kluwer Academic Publishers Group, Dordrecht, 1996.
9. C. W. Groetsch, *The Theory of Tikhonov Regularization for Fredholm Equations of the First Kind*, Pitman, Boston, 1984.
10. M. Hanke, *Conjugate Gradient Type Methods for Ill-Posed Problems*, Longman Scientific & Technical, Harlow, 1995. <https://doi.org/10.1201/9781315140193>
11. B. Kaltenbacher, A. Neubauer, O. Scherzer, *Iterative Regularization Methods for Nonlinear Ill-Posed Problems*, Walter de Gruyter, Berlin, 2008. <https://doi.org/10.1515/9783110208276>

12. L. I. Rudin, S. Osher, E. Fatemi, Nonlinear total variation based noise removal algorithms, *Physica D*, **60** (1992), 259–268. [https://doi.org/10.1016/0167-2789\(92\)90242-F](https://doi.org/10.1016/0167-2789(92)90242-F)
13. G. Bao, S. Hou, P. Li, Recent studies on inverse medium scattering problems, in *Modeling and Computations in Electromagnetics*, (2008), 165–186. https://doi.org/10.1007/978-3-540-73778-0_6
14. K. Ito, B. Jin, T. Takeuchi, Multi-parameter Tikhonov regularization, *Methods Appl. Anal.*, **18** (2011), 31–46. <https://doi.org/10.4310/MAA.2011.v18.n1.a2>
15. M. V. Klibanov, J. Li, *Inverse Problems and Carleman Estimates: Global Uniqueness, Global Convergence and Experimental Data*, De Gruyter, Berlin, 2021. <https://doi.org/10.1515/9783110745481>
16. O. Y. Imanuvilov, M. Yamamoto, Carleman estimate and an inverse source problem for the Kelvin-Voigt model for viscoelasticity, *Inverse Probl.*, **35** (2019), 125001. <https://doi.org/10.1088/1361-6420/ab323e>
17. Y. Jia, J. Yang, Determination of embedded obstacle and its surrounding medium in electrostatics, *Inverse Probl.*, **41** (2025), 065008. <https://doi.org/10.1088/1361-6420/add75e>
18. D. Zhang, Y. Chang, Y. Guo, Jointly determining the point sources and obstacle from Cauchy data, *Inverse Probl.*, **40** (2024), 015014. <https://doi.org/10.1088/1361-6420/ad10c8>
19. D. Zhang, Y. Wu, Y. Guo, Imaging an acoustic obstacle and its excitation sources from phaseless near-field data, *Inverse Probl. Imaging*, **18** (2024), 797–812. <https://doi.org/10.3934/ipi.2023055>
20. H. Wu, J. Yang, J. Li, The factorization method for simultaneous reconstruction of a piecewise homogeneous medium and a buried object from near-field data, *Inverse Probl.*, **41** (2025), 065007. <https://doi.org/10.1088/1361-6420/addb6b>
21. S. J. Norton, Generation of separate density and compressibility images in tissue, *Ultrason. Imaging*, **5** (1983), 240–252. [https://doi.org/10.1016/0161-7346\(83\)90004-4](https://doi.org/10.1016/0161-7346(83)90004-4)
22. J. Virieux, S. Operto, An overview of full-waveform inversion in exploration geophysics, *Geophysics*, **74** (2009), WCC1–WCC26. <https://doi.org/10.1190/1.3238367>
23. S. Operto, Y. Gholami, V. Prioux, A. Ribodetti, R. Brossier, L. Metivier, et al., A guided tour of multiparameter full-waveform inversion with multicomponent data: From theory to practice, *Geophysics*, **32** (2013), 1040–1054. <https://doi.org/10.1190/tle32091040.1>
24. Y. Gholami, R. Brossier, S. Operto, A. Ribodetti, J. Virieux, Which parametrization is suitable for acoustic VTI full-waveform inversion? Part 1: sensitivity and trade-off analysis, *Geophysics*, **78** (2013), R81–R105. <https://doi.org/10.1190/geo2012-0204.1>
25. K. Ito, B. Jin, T. Takeuchi, Multi-parameter Tikhonov regularization—an augmented approach, *Chin. Ann. Math. Ser. B*, **35** (2014), 383–398. <https://doi.org/10.1007/s11401-014-0835-y>
26. J. Xu, J. Huang, A. Chen, Representation of a class of linear operators with coupled domain in a product space and its applications, *Acta Math. Sin.*, **39** (2023), 326–338. <https://doi.org/10.1007/s10114-023-1387-4>
27. J. Xu, J. Huang, A. Chen, Analyticity and stability of semigroups related to an abstract initial-boundary value problem, *Oper. Matrices*, **17** (2023), 549–565. <https://doi.org/10.7153/oam-2023-17-36>

28. J. Xu, J. Huang, A. Chen, Fredholm properties of a class of coupled operator matrices and their applications, *Ann. Funct. Anal.*, **15** (2024), 12. <https://doi.org/10.1007/s43034-024-00318-z>
29. A. Kirsch, *An Introduction to the Mathematical Theory of Inverse Problems*, Springer, Cham, 2021. <https://doi.org/10.1007/978-3-030-63343-1>
30. C. R. Vogel, *Computational Methods for Inverse Problems*, SIAM, Philadelphia, 2002. <https://doi.org/10.1137/1.9780898717570>
31. T. Kato, *Perturbation Theory for Linear Operators*, Springer, Berlin, 1995. <https://doi.org/10.1007/978-3-642-66282-9>
32. A. Ben-Israel, T. N. E. Greville, *Generalized Inverses: Theory and Applications*, Springer, New York, 2003. <https://doi.org/10.1007/b97366>
33. C. Y. Deng, H. K. Du, Representations of the Moore-Penrose inverse of 2×2 block operator valued matrices, *J. Korean Math. Soc.*, **46** (2009), 1139–1150. <https://doi.org/10.4134/JKMS.2009.46.6.1139>



AIMS Press

©2026 the Author(s), licensee AIMS Press. This is an open access article distributed under the terms of the Creative Commons Attribution License (<https://creativecommons.org/licenses/by/4.0>)